

Quantum State Preparation via Large-Language-Model-Driven Evolution

Qing-Hong Cao,^{1,2,*} Zong-Yue Hou,^{1,†} Ying-Ying Li,^{3,‡} Xiaohui Liu,^{4,5,§}
Zhuo-Yang Song,^{1,¶} Liang-Qi Zhang,^{1,**} Shutao Zhang,^{1,††} and Ke Zhao^{1,‡‡}

¹*School of Physics, Peking University, Beijing 100871, China*

²*Center for High Energy Physics, Peking University, Beijing 100871, China*

³*Institute of High Energy Physics, Chinese Academy of Sciences, Beijing 100049, China*

⁴*Center of Advanced Quantum Studies, School of Physics and Astronomy,
Beijing Normal University, Beijing, 100875, China*

⁵*Key Laboratory of Multi-scale Spin Physics, Ministry of Education,
Beijing Normal University, Beijing 100875, China*

We propose an automated framework for quantum circuit design by integrating large-language models (LLMs) with evolutionary optimization to overcome the rigidity, scalability limitations, and expert dependence of traditional ones in variational quantum algorithms. Our approach (FunSearch) autonomously discovers hardware-efficient ansätze with new features of scalability and system-size-independent number of variational parameters entirely from scratch. Demonstrations on the Ising and XY spin chains with $n = 9$ qubits yield circuits containing 4 parameters, achieving near-exact energy extrapolation across system sizes. Implementations on quantum hardware (Zuchongzhi chip) validate practicality, where two-qubit quantum gate noises can be effectively mitigated via zero-noise extrapolations for a spin chain system as large as 20 sites. This framework bridges algorithmic design and experimental constraints, complementing contemporary quantum architecture search frameworks to advance scalable quantum simulations.

Introduction. Efficient preparation of correlated many-body quantum states is critical for near-term applications in physics [1], quantum chemistry [2], and combinatorial optimization [3–5], however remains a fundamental bottleneck for noisy intermediate-scale quantum (NISQ) [1] hardware. Variational quantum algorithms (VQAs) [6–8] and their machine-learning extensions typically rely on manually crafted ansatz circuits with limited variations of circuit architectures, which often require deep gates and a large number of parameters to be optimized. These ansätze can lead to barren plateaus in optimization landscapes [9], and depend heavily on expert intuition that hinders scalability across problems. Tremendous efforts have been made to overcome these limitations; see [10] for a review.

In this work, we propose applying the FunSearch framework [11] that integrates a large-language model (LLM) with evolutionary optimization to autonomously design and refine ansatz circuits. Starting from *generic, physics-agnostic* templates, the framework iteratively generates candidate circuits through a feedback-driven loop: candidates are evaluated by a cost balancing expectation value accuracy and circuit complexity, and the top performers seed genetic-algorithm mutations and crossovers.

We validate this approach on two paradigmatic spin chain models. For the transverse field Ising chain of 9 sites corresponding to 9 qubits, the framework quickly discovers an 8-layer, 4-parameter circuit achieving a ground state fidelity $F = 0.982$ and an error in the ground state energy E to be less than 0.3%. Similar success for the anisotropic XY model with 9-qubits yields a 5-layer and 4-parameter circuit featuring spatially mod-

ulated rotations that implicitly adapt to open boundary conditions, achieving a fidelity $F = 0.98$ and an error in E to be less than 0.4%. Remarkably, both ansätze extrapolate to 35 qubits with less than 0.7% errors in E . The resulting circuits use rotation and CNOT gates, natively executable with minimal overhead on quantum computing platforms, ensuring hardware efficiency. In contrast, during the optimization process, we observed that the LLM generates circuits employing unrestricted gates, such as the S gate and the CCX (Toffoli) gate. The observation shows that the LLM-driven evolution autonomously prioritizes ansätze that are hardware and optimization efficient, featuring a system-size-independent number of variational parameters adherent to physical principles. This also ensures that all designs remain NISQ-compatible without quantum-hardware architectural prescriptions.

Automated Ansatz Discovery. We apply FunSearch, originally developed for mathematical optimization [11], to automate physics-aware quantum circuit synthesis. The central objective is to efficiently prepare a target quantum state, by minimizing the functional $C_O[\psi(\theta)] = \langle \psi(\theta) | O | \psi(\theta) \rangle$, where $|\psi(\theta)\rangle$ represents a parameterized ansatz circuit, and O is the problem-specific operator (e.g., Hamiltonian, projector) whose minimization ensures convergence to the desired state.

Figure 1 outlines the iterative workflow:

1. LLMs iteratively propose ansatz candidates from physics-agnostic templates [12], with unlimited gate pools.
2. Candidates are optimized variationally to minimize $C_O[\psi(\theta)]$, and scored [12] using a metric that balances the minimal value of $C_O[\psi(\theta)]$ and circuit complexity.

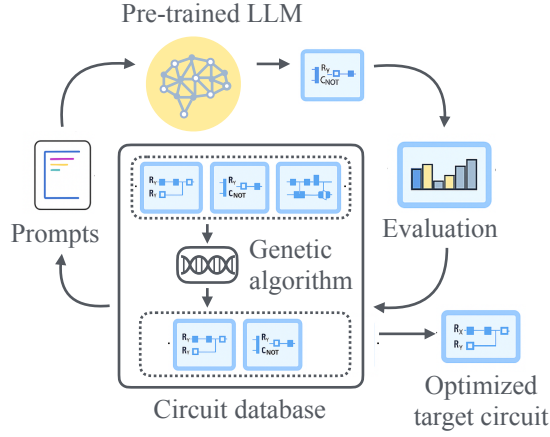


FIG. 1. Integrated workflow for quantum ansatz design.

3. Top-performing candidates seed a genetic algorithm [11, 12] that applies mutations and crossovers, ensuring diversity while escaping local optima, to evolve the circuit database. At any time, the user can retrieve the highest score ansatz as the optimized circuit.

This automated workflow requires no manual ansatz tailoring: all physical insight, such as boundary-condition sensitivity or symmetry exploitation, emerges organically through the LLM’s iterative refinement under the evolutionary selection. In the following sections, we apply this protocol to benchmark Ising and XY spin chain models, demonstrating its rapid convergence to compact, high-fidelity circuits scalable to larger system sizes.

The Ising Model. We first demonstrate our framework by preparing the ground state of the transverse-field Ising chain:

$$H_{\text{Ising}} = - \sum_{i=1}^{n-1} \sigma_i^z \sigma_{i+1}^z - g_x \sum_i \sigma_i^x. \quad (1)$$

with $n = 9$, $g_x = 1$, and open boundary conditions. The objective is to minimize the energy expectation $C_{H_{\text{Ising}}}[\psi(\theta_i)] = \langle \psi(\theta_i) | H_{\text{Ising}} | \psi(\theta_i) \rangle \equiv E$.

Using the DeepSeek-Distill-Qwen-32B [13] LLM at model temperature 1.0, the framework identifies an optimal ansatz within 100 hours (Fig. 2), with a ground state fidelity $F = 0.982$ and the error in the ground state energy $|\Delta E/E| < 0.3\%$, showcasing the framework’s effectiveness despite minimal prior physical insight.

The time evolution shown in Fig. 2 exhibits the searching stage based on knowledge and refining stage to add new features originated from the creativity of LLM in the process to design the optimal circuit. With prior knowledge, LLM quickly identifies the hardware-efficient ansatz with $\mathcal{O}(n)$ free variational parameters [14] and the first drop in ΔE happens. Then LLM starts refining the structure of circuits, as well as refining the patterns of the variational parameters without relying on prior

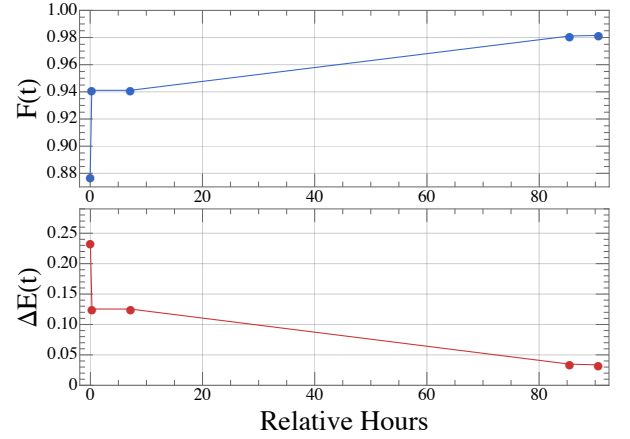


FIG. 2. Time evolution of the highest-scoring ansatz found by the FunSearch.

knowledge of existing ansätze, which takes a reasonably longer time. During this process, ansätze that are prone to barren plateaus or exhibit inefficient optimization in VQA can be discarded.

The optimal circuit exhibits a simple architecture: it requires only 4 parameters, and 8 layers of operation exclusively employing R_Y rotations and CNOT gates (Fig. 3). For comparisons, Ref. [15] utilized a circuit with $\mathcal{O}(20)$ gate layers and $\mathcal{O}(20)$ parameters to attain comparable fidelity, while using the fidelity optimization, instead of the energy-based approach in our demonstration, to avoid local optima. Ref. [16] reported a semi-agnostic architecture search result achieving a better energy error for $n = 8$ with $\mathcal{O}(30)$ parameters.

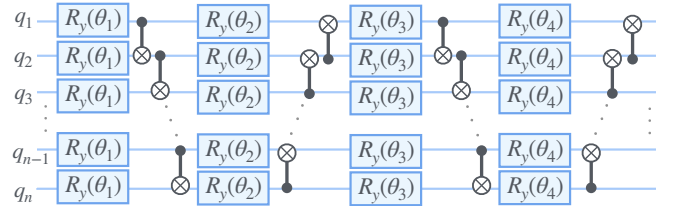


FIG. 3. Best-scoring ansatz found by the framework in 100 hours for the $n = 9$ Ising model.

The simplicity of the ansatz enables scalable extrapolation. Keeping the architecture fixed, we use VQA to determine the optimized parameter values for $n = 4$ to $n = 10$. By fitting the optimized parameters $\theta_1, \dots, \theta_4$ to smooth functions (Fig. 4), we extend the circuit to systems up to $n = 35$. For $n > 14$, we obtain the ground states prepared with the extrapolated circuits by tensor network methods using quimb [17]. Fig. 5 shows near-exact agreement between extrapolated and exact ground-state energies, with $|\Delta E/E| < 0.5\%$ across all n considered. We also show the single-qubit fidelity $F_s = \sqrt[n]{F}$ in Fig. 6. We observe that F_s remains $\gtrsim 0.995$ for $n \lesssim 20$, which, together with the small $|\Delta E/E|$ across all system sizes up to $n = 35$, demonstrates robust accuracy of the

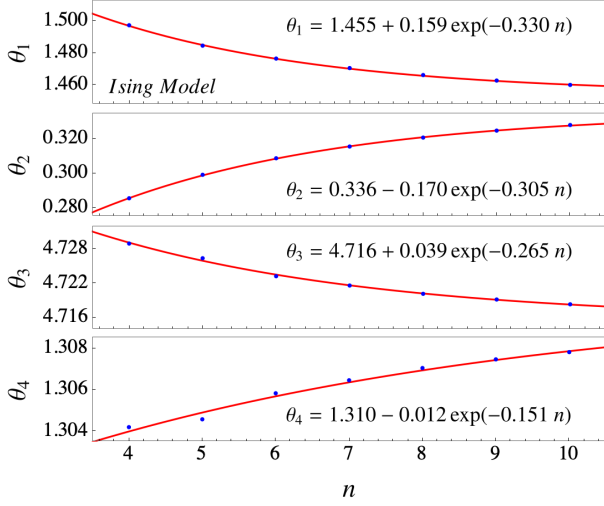


FIG. 4. Optimal parameters θ_1 - θ_4 derived from energy minimization for the ansatz in Fig. 3. These parameters exhibit a clear trend towards asymptotic stability (the boundary effects of the ansatz diminish with increasing qubit number n in the qubit chain). The blue dots represent the optimal parameters obtained using VQA in qiskit as a function of the number of qubits n . The red lines are fits to these parameters.

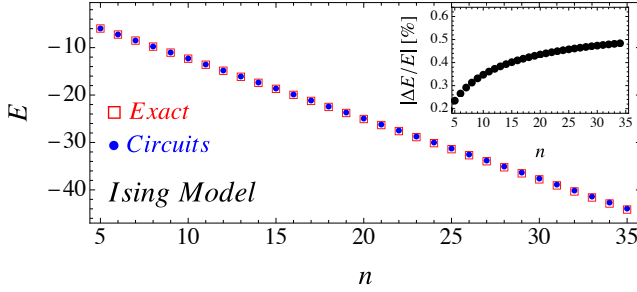


FIG. 5. The ground state energy with different sizes. The blue dots represent the energy of the prepared ground state by circuits with the fitting parameters from Fig. 4, while the red boxes represent the exact energy of the ground state. The subfigure illustrates the relative difference of the prepared state energy with the ground state energy.

extrapolated circuits.

Note that our optimization relies solely on minimizing the energy of the states. Fidelity could be further improved through multi-objective optimization strategies that explicitly incorporate quantum state fidelities or symmetry preservation.

The XY Model. To validate the versatility, we apply the framework to the anisotropic XY spin chain:

$$H_{XY} = \sum_i^{n-1} \left(\frac{1+\gamma}{2} \sigma_i^x \sigma_{i+1}^x + \frac{1-\gamma}{2} \sigma_i^y \sigma_{i+1}^y \right) + g_z \sum_i^n \sigma_i^z, \quad (2)$$

with $n = 9$, $g_z = 1.0$, $\gamma = 1.0$, and open boundary con-

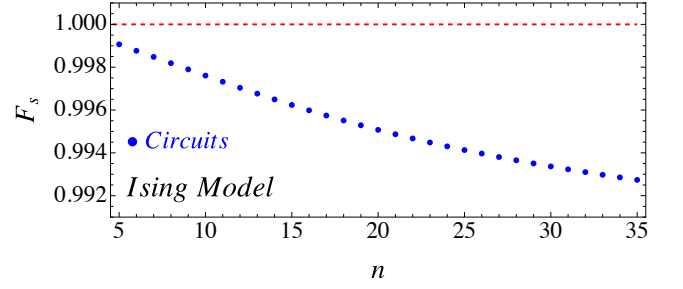


FIG. 6. The single-qubit fidelity F_s as a function of the number of qubits n . The blue dots represent the results obtained using MPS and parameter extrapolation on the ansatz in Fig. 3. The red dashed line indicates the ideal case where $F_s = 1$.

dition. Using the same protocol as for the Ising model, the framework identifies an optimal ansatz (Fig. 7) in 24 hours, comprising only 5 layers and 4 tunable parameters, achieving a ground state fidelity $F = 0.96$, see details in the Supplemental materials [12].

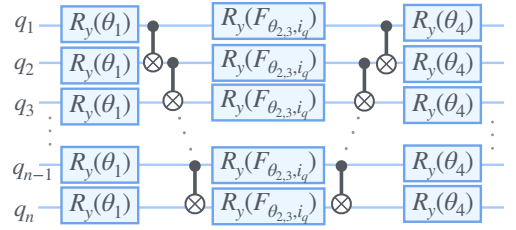


FIG. 7. Best ansatz returned by our strategy with the circuit depth of 5 and 4 free parameters.

A noteworthy feature is the framework's preferential use of a spatially modulated local rotation (Fig. 7, Layer 3):

$$F_{\theta_{2,3}, i_q} = \theta_2 + \theta_3 \cdot \sin \left(\frac{i_q + 1}{n} \pi \right), \quad (3)$$

where $i_q = 0, 1, \dots, n-1$ indicates the qubit location in the system. Peaking around $i_q = 0$ and $n-1$, this modulation enhances rotations near the chain boundary, with a stronger effect at $n-1$, thereby implicitly encoding open boundary conditions. With the emergent spatial modulation featuring the boundary conditions of the system, we are inspired to propose the refined rotations

$$F_{\theta_{2,3}, i_q}^h = \theta_2 + \theta_3 \cdot \cos^{2n} \left(\frac{i_q + 1}{n} \pi \right), \quad (4)$$

to sharpen the boundary gradient and improve the overall circuit performance. The ability of LLMs to spark novel human insights creates a dynamic feedback loop where machine-generated suggestions and human expertise mutually reinforce each other, forming a cognitive synergy that merits systematic investigation in the future.

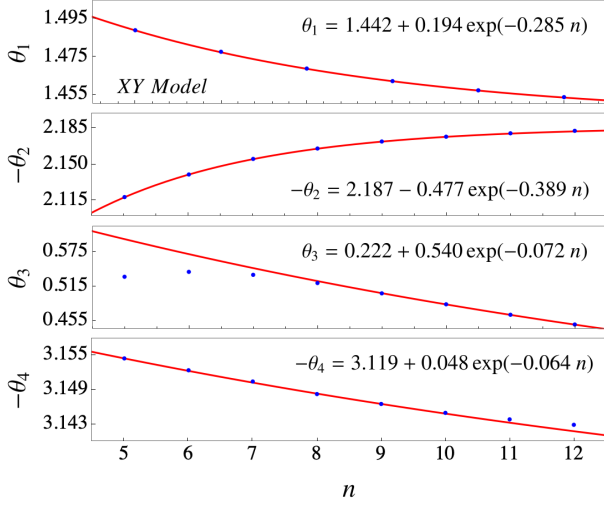


FIG. 8. Optimal parameters θ_1 - θ_4 derived from energy minimization for the ansatz in Fig. 7.

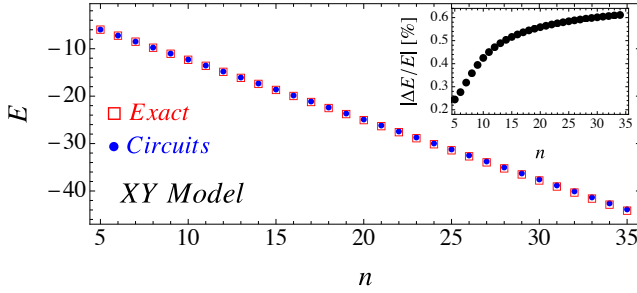


FIG. 9. Energy extrapolation for the XY model. We adopt the same plot setting as in Fig. 5

The compact ansatz architecture enables scalable generalization across system sizes. To validate this, we again extrapolate the circuit to varying n by fitting the optimized parameters θ from VQA performed from $n = 4$ to 12, as shown in Fig. 8. For θ_3 , the fit is performed without including results from $n = 5$ and $n = 6$, given the large effects from finite sizes unsuitable to achieve reliable extrapolation. The energy of the prepared states using extrapolated circuits in comparison to that of the ground state and the single-qubit fidelity F_s are shown in Fig. 9 and Fig. 10, respectively. We observe that $|\Delta E/E|$ remains below 0.7%, while $F_s > 0.995$ for $n \lesssim 20$, confirming again the scalability of the quantum circuits found by LLMs.

Demonstration on Quantum Hardware. We executed the XY model ($\gamma = 1.0$) circuits on the Zuchongzhi quantum chip [18] to demonstrate the practicality of state preparation for small systems in the NISQ era. We select a chain of qubits where the singlet-qubit gate can be applied with fidelity higher than 99.5% and two-qubit gates higher than 98%, which are the qubits connected by

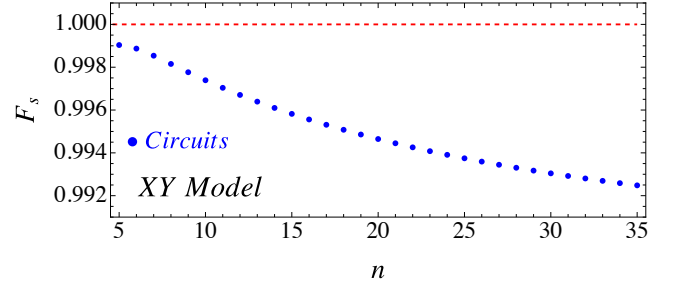


FIG. 10. Single-qubit fidelity F_s as a function of the system size n .

green solid lines of the Zuchongzhi architecture shown in the top panel of Fig. 11. For various systems of n qubits chosen from the chain, we run the XY model ($\gamma = 1.0$) circuits, which is identified as noise strength $\mathcal{N}_s = 1$, and measure the energy of the final states. To mitigate quantum noises from the imperfect CNOT gates using the Zero Noise Extrapolation (ZNE) [19, 20] method, we adopt the following strategy. We amplify \mathcal{N}_s by replacing a single CNOT gate with three sequential CNOT gates, which are equivalent in the absence of quantum noise. Running these circuits with different \mathcal{N}_s and obtaining the energy of the corresponding final states, the quantum noise can be reduced by extrapolating to the $\mathcal{N}_s = 0$ case, with the extrapolation details reserved to the Supplemental materials [12].

Figure 11 shows the extrapolated energy using an exponential fit, quadratic fit and linear fit with the 1σ fitting uncertainties (top panel), as well as the χ^2/dof values for each fitting function (bottom panel). The energy from a noiseless case using a quantum simulator for the corresponding circuit is shown as white solid circles in the top panel. Although the exponential fit yields a reduced chi-squared of order unity $\chi^2/dof \sim 1$, the diagonal elements of its covariance matrix are significantly larger than 1. This suggests that the exponential model may be overparameterized, and the fitting should be degraded. A similar issue arises in the case of the quadratic fit, where $\chi^2/dof \ll 1$ also indicates potential overfitting or overparameterization. The linear fit instead provides a much better representation of the data in the range $n = 10$ to $n = 20$. In particular, the extrapolated energies from the linear fit agree with the noiseless values within one standard deviation for $n = 10$. For $n = 12, n = 15$ and $n = 20$, the discrepancies remain below 15%, 20% and 30%, respectively. These discrepancies are found to match the estimated unmitigated errors arising from single-qubit gate imperfections, given by $1 - 0.995^{3n}$, where 0.995 is the maximal single-qubit gate fidelity and $3n$ is the number of single-qubit gates in the circuit.

Conclusion and Outlook. This manuscript initiates a study on the efficacy and versatility of an LLM-

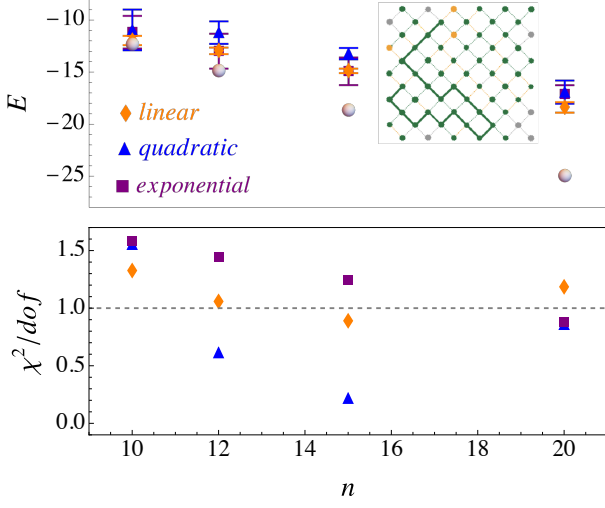


FIG. 11. (top) Extrapolated energy of the states prepared on Zuchongzhi quantum chip for n qubits, using exponential fit (purple square), quadratic fit (blue triangle) and linear fit (orange diamond). The white solid circle is obtained from a noiseless quantum simulator. The architecture of Zuchongzhi chip is also shown in the upper corner. (bottom) The χ^2/dof in each fit. The dashed horizontal is for $\chi^2/\text{dof} = 1$.

driven framework (FunSearch) for assisting quantum circuit design. By integrating LLMs with physics-aware evolutionary optimization, our approach systematically circumvents the limitations of manual ansatz construction in variational quantum algorithms. The framework successfully identifies high-fidelity circuit architectures for the Ising and XY spin chains, with remarkably fewer parameters and layers than conventional methods. Crucially, these results were obtained with minimal human intervention: both initial ansätze and gate pools were deliberately stripped of physical intuition (e.g., symmetry constraints), and optimization prioritized energy minimization. This strict validation protocol underscores the framework’s inherent ability to autonomously infer physical constraints (e.g., boundary conditions) and compensate for operational asymmetries (e.g., CNOT gate biases) through iterative feedback.

The current implementation prioritizes scalability and hardware compatibility, intentionally limiting parameter counts, a trade-off that preserves extrapolation accuracy while leaving room for fidelity gains in fixed-size applications. Future work could enhance performance through symmetry-aware prompts, hybrid energy-fidelity metrics, or meta-learning for accelerated evolution. In addition, this work focuses on 1-D spin chains as a foundational testbed; future research will target geometrically complex systems such as scalar field or gauge field models in higher spatial dimensions, whose state preparation is part of the critical components for tackling longstanding challenges in high energy physics by quantum comput-

ing [21–25].

Furthermore, our methodology can be integrated with contemporary quantum architecture search frameworks, for instance, to automate the generation of the gate/operator pools, a keystone of most architecture search algorithms [16, 26]. Such a hybrid paradigm would merge the creativity of AI-driven exploration with the robustness of domain-specific heuristics, potentially achieving superior performance.

Beyond state preparation, this methodology exhibits versatile applicability to design challenges across fields. The ability to autonomously synthesize hardware-efficient, physics-compliant architectures generalizes naturally to problems such as quantum error correction code design, tensor network optimization, or even experimental apparatus configuration. By liberating researchers from iterative trial-and-error cycles, this framework opens new pathways for AI-driven discovery in quantum technologies and fundamental science.

Acknowledgements. We thank Xu Feng, Futian Liang, Xiaoyang Wang, Zhi-Cheng Yang, and Xiao Yuan for fruitful discussions. The authors gratefully acknowledge the valuable discussions and insights provided by the members of the Collaboration on Precision Tests and New Physics (CPTNP). The work is partly supported by the National Science Foundation of China under Grant Nos. 12235001, 12175016, 12425505, 12305107. This work was also partly supported by Tianyan Quantum Computing Cloud Platform.

* qinghongcao@pku.edu.cn

† zongyuehou@stu.pku.edu.cn

‡ liyingying@ihep.ac.cn

§ xiliu@bnu.edu.cn

¶ zhuoyangsong@stu.pku.edu.cn

** liangqizhang@pku.edu.cn

†† shutaozhang@pku.edu.cn

‡‡ ke-zhao@pku.edu.cn

- [1] J. Preskill, *Quantum* **2**, 79 (2018), 1801.00862.
- [2] D. Wecker, B. Bauer, B. K. Clark, M. B. Hastings, and M. Troyer, *Phys. Rev. A* **90**, 022305 (2014).
- [3] M. P. Harrigan *et al.*, *Nature Phys.* **17**, 332 (2021), 2004.04197.
- [4] S. Ebadi *et al.*, *Science* **376**, 1209 (2022), 2202.09372.
- [5] Y. Zhu *et al.*, *Sci. Bull.* **70**, 460 (2025).
- [6] J. R. McClean, J. Romero, R. Babbush, and A. Aspuru-Guzik, *New J. Phys.* **18**, 023023 (2016), 1509.04279.
- [7] E. Farhi, J. Goldstone, and S. Gutmann, (2014), 1411.4028.
- [8] M. Cerezo *et al.*, *Nature Rev. Phys.* **3**, 625 (2021), 2012.09265.
- [9] J. R. McClean, S. Boixo, V. N. Smelyanskiy, R. Babbush, and H. Neven, *Nature Commun.* **9**, 4812 (2018), 1803.11173.
- [10] D. Martyniuk, J. Jung, and A. Paschke, *Quantum Architecture Search: A Survey*, in *2024 International Con-*

- ference on Quantum Computing and Engineering*, 2024, 2406.06210.
- [11] B. Romera-Paredes *et al.*, *Nature* **625**, 468 (2024).
 - [12] Supplemental material for “quantum state preparation via llm-driven evolution”, 2025.
 - [13] DeepSeek-AI, Deepseek-r1: Incentivizing reasoning capability in llms via reinforcement learning, 2025, 2501.12948.
 - [14] A. Peruzzo *et al.*, *Nature Communications* **5**, 4213 (2014).
 - [15] H. Xu *et al.*, *Phys. Rev. Lett.* **134**, 120803 (2025), 2503.02210.
 - [16] M. Bilkis, M. Cerezo, G. Verdon, P. J. Coles, and L. Cincio, *Quantum Machine Intelligence* **5**, 43 (2023), 2103.06712.
 - [17] J. Gray, *Journal of Open Source Software* **3**, 819 (2018).
 - [18] Q. Zhu *et al.*, *Sci. Bull.* **67**, 240 (2022), 2109.03494.
 - [19] K. Temme, S. Bravyi, and J. M. Gambetta, *Phys. Rev. Lett.* **119**, 180509 (2017), 1612.02058.
 - [20] Y. Li and S. C. Benjamin, *Phys. Rev. X* **7**, 021050 (2017), 1611.09301.
 - [21] C. W. Bauer *et al.*, *PRX Quantum* **4**, 027001 (2023), 2204.03381.
 - [22] A. Di Meglio *et al.*, *PRX Quantum* **5**, 037001 (2024), 2307.03236.
 - [23] C. W. Bauer, Z. Davoudi, N. Klco, and M. J. Savage, *Nature Reviews Physics* **5**, 420 (2023).
 - [24] Y. Fang *et al.*, *Sci. China Phys. Mech. Astron.* **68**, 260301 (2025), 2411.11294.
 - [25] C. W. Bauer, Z. Davoudi, N. Klco, and M. J. Savage, *Nature Rev. Phys.* **5**, 420 (2023), 2404.06298.
 - [26] R. C. Farrell, M. Illa, A. N. Ciavarella, and M. J. Savage, *PRX Quantum* **5**, 020315 (2024), 2308.04481.
 - [27] F. Liu *et al.*, Evolution of heuristics: Towards efficient automatic algorithm design using large language model, 2024, 2401.02051.

Supplemental Material for “Quantum State Preparation via LLM-Driven Evolution”

A. Additional Details on the Methodology

To illustrate the efficiency of our results, we deployed our model on a single NVIDIA A800 GPU without concurrency. Additionally, when optimizing the circuit parameters through brute-force calculations, we used the Intel(R) Xeon(R) Platinum 8358P CPU @ 2.60GHz, and concurrency was also not employed.

We elaborate on the technical details of the evolution, evolutionary score, and initial ansatz of the framework.

- *Evolution:* The genetic algorithm used in FunSearch employs an island-based model to maintain a diverse population of programs and escape local optima. Each island evolves independently, and periodically, the islands with the lowest scores are reset with programs from the highest-performing islands. This method ensures diversity and prevents the algorithm from getting stuck in local optima. The initial programs are sampled from the programs database, and the LLM generates new programs based on these samples. The new programs are then evaluated and added to the island, either in an existing cluster or a new one if its signature is not yet present. This process is repeated until termination [11]. Natural language prompt giving a few shots was adapted since it has been proven effective [27].
- *Prompt Template:* The routine to generate the prompt template is given in Listing 1.

Listing 1. Routine that generates the prompt.

```

1 def _build_prompt(self, examples):
2     """Build a code generation prompt containing examples"""
3     problem_desc = (
4         r"</think>"
5         "The user's requirement is to generate a suitable quantum circuit ansatz with as few parameters
6         ↳ as possible, so that it can be easily extended to a multi-qubit system while still
7         ↳ being effective."
8         "<We are attempting to generate an ansatz and optimize it variationally to find the most
9         ↳ suitable quantum circuit for preparing the initial state of an ising theory>\n\n"
10
11         "Function framework to be implemented:\n"
12         "from qiskit import QuantumCircuit, transpile\n"
13         "from qiskit.circuit import Parameter, ParameterVector\n"
14         f"def {self.config.TARGET_FUNCTION}:\n"
15         "\t# This should be the implementation of the ansatz\n"
16     )
17
18     existing_code = (
19         "#def do_vqe():\n"
20         "\tvqe = VQE(estimator=estimator, ansatz=qc_ansatz, optimizer=optimizer, callback=callback)\n"
21         "\tresult = vqe.compute_minimum_eigenvalue(operator=H)\n"
22         "\treturn result.eigenvalue\n"
23         "# Other related function structures...\n"
24     )
25
26     examples_section = "\n".join(
27         [f"#ExampleCode_{i+1}:\n{example}"
28          for i, example in enumerate(examples)]
29     )
30
31     requirements = (
32         "\n#Generation Requirements:\n"
33         "#1. The function must be correctly defined\n"
34         "#2. The output of the function should be physically reasonable (entanglement, rotation, etc.)
35         ↳ \n"
36         "#3. Do not directly copy the examples, and at least complete one of the following (generalize
37         ↳ the previous code, simplify the previous code, evolve the previous code, create a
38         ↳ unique implementation)\n"
39         "#4. Ensure that the code includes the necessary mathematical operation library imports\n"
40         "#5. Pay attention to the simplicity and scalability of the code parameters\n"
41         "#6. Wrap the final code in a Python code block\n"

```

```

36         r"</answer>"
37     )

```

- *Evolutionary score:* The evolutionary score is determined using a function that incorporates the energy change ΔE and a temperature parameter $T = 0.5$. The score update mechanism is based on the Boltzmann selection procedure, which introduces a probabilistic component to the scoring. Specifically, the score update ΔS is calculated as follows:

$$\Delta S = -\frac{\Delta E}{T}, \quad (5)$$

where ΔE is the change in energy between the current solution and the previous solution. $T = 0.5$ is the temperature parameter that controls the sensitivity of the score to energy changes.

The probability P of accepting a new solution is given by

$$P = \exp\left(-\frac{\Delta E}{T}\right), \quad (6)$$

which ensures that solutions with lower energy changes are more likely to be accepted, while still allowing for exploration of higher energy solutions, to help escape local optima [11].

Besides, we restrict the number n_p of tunable parameters to be small by forcing the evaluator to erase any circuits with $n_p > 9$. No constraint on the circuit depth is imposed for the time being.

- *Initial ansatz:* The initial ansatz in `python` is shown in Listing 2

Listing 2. Initial ansätze

```

1  # --- Initial Ansatz I ---
2  def create_ansatz(n):
3      qc = QuantumCircuit(n)
4      params = ParameterVector('params', 2)
5      for qubit in range(n):
6          qc.rx(params[0]+params[1]*qubit/n, qubit)
7      return qc
8
9  # --- Initial Ansatz II ---
10 def create_ansatz(n):
11     qc = QuantumCircuit(n)
12     params = ParameterVector('params', 3)
13     for qubit in range(n):
14         qc.ry(params[qubit//3], qubit)
15     return qc
16
17 # --- Initial Ansatz III ---
18 import numpy as np
19 def create_ansatz(n):
20     qc = QuantumCircuit(n)
21     params = ParameterVector('params', 2)
22     for qubit in range(n):
23         qc.rz(params[0]+np.exp(params[1]), qubit)
24     return qc

```

Note that the choice of the initial ansatz is arbitrary. Our initial ansatz selection deliberately avoids incorporating domain-specific insights to rigorously evaluate our framework's exploration capabilities. While expert-designed ansätze typically employ symmetry-aware parameterization to accelerate convergence, we instead implement architecturally distinct circuits containing no a priori physical constraints. This strategic choice eliminates human bias in circuit architecture selection, forcing the algorithm to discover optimized ansatz through pure optimization dynamics.

B. Evolutionary History for the XY Model

Fig. 12 presents the evolution history. We see that within 24 hours running, the framework comes up with a high-fidelity ansatz with $F = 0.96$ and the relative difference between the minimized energy and the exact ground state energy is less than 1%.

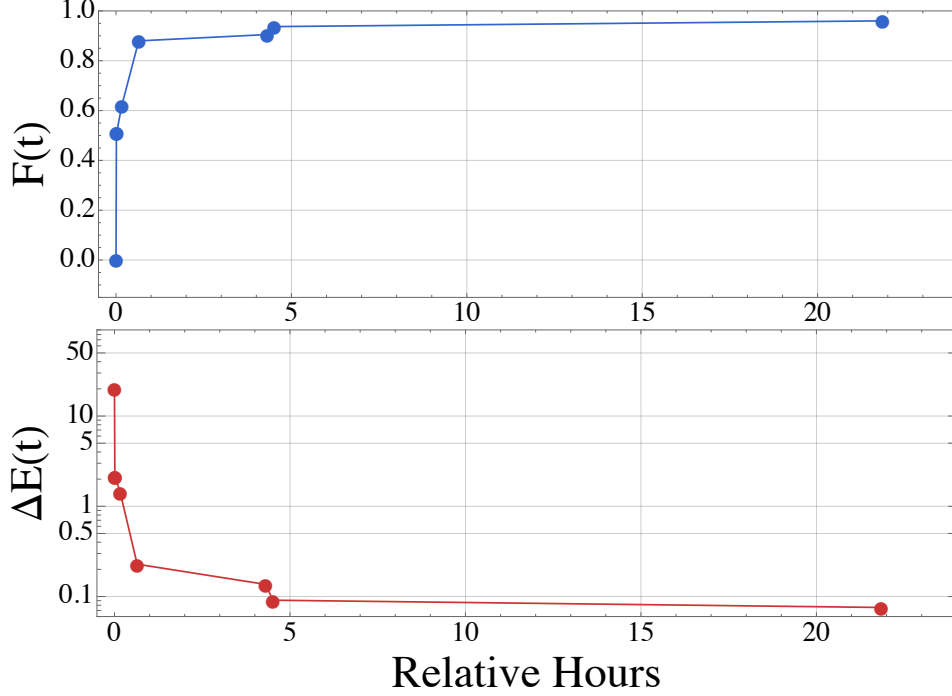


FIG. 12. Evolution of the highest-scoring ansatz for the XY model with $n = 9$, $\gamma = 1.0$ and $g_x = 1.0$.

Fig. 13 shows an exemplary circuit generated by LLM with a lower score, whose ground energy error is of order 5%.

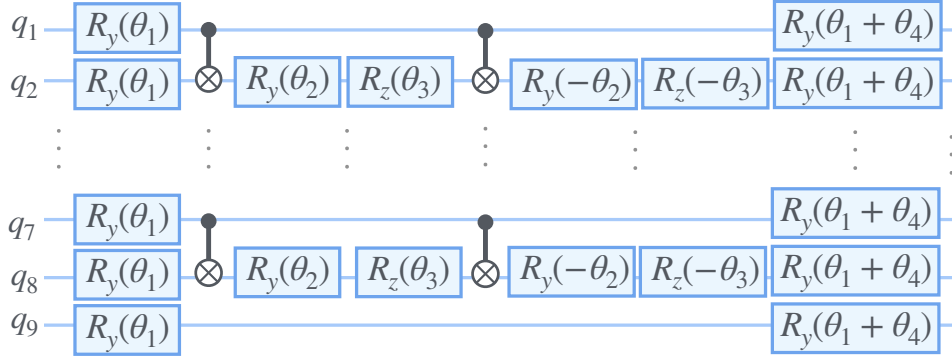


FIG. 13. An exemplary circuit generated by LLM with a low score.

C. Additional details about experiments on quantum hardware

We executed the XY model ($\gamma = 1.0$) circuits on the Zuchongzhi quantum chip [18]. In the experiment, we selected five systems of different sizes, corresponding to $n = 10, 12, 15, 20$, respectively. We consider the initial circuit's noise strength to be 1, and vary the circuit's noise strength by replacing a single CNOT gate with three or five CNOT gates. For a system of size n , we define noise strength as $\mathcal{N}_s = N_{\text{CNOT}}/(2n - 2)$, where N_{CNOT} is the number of

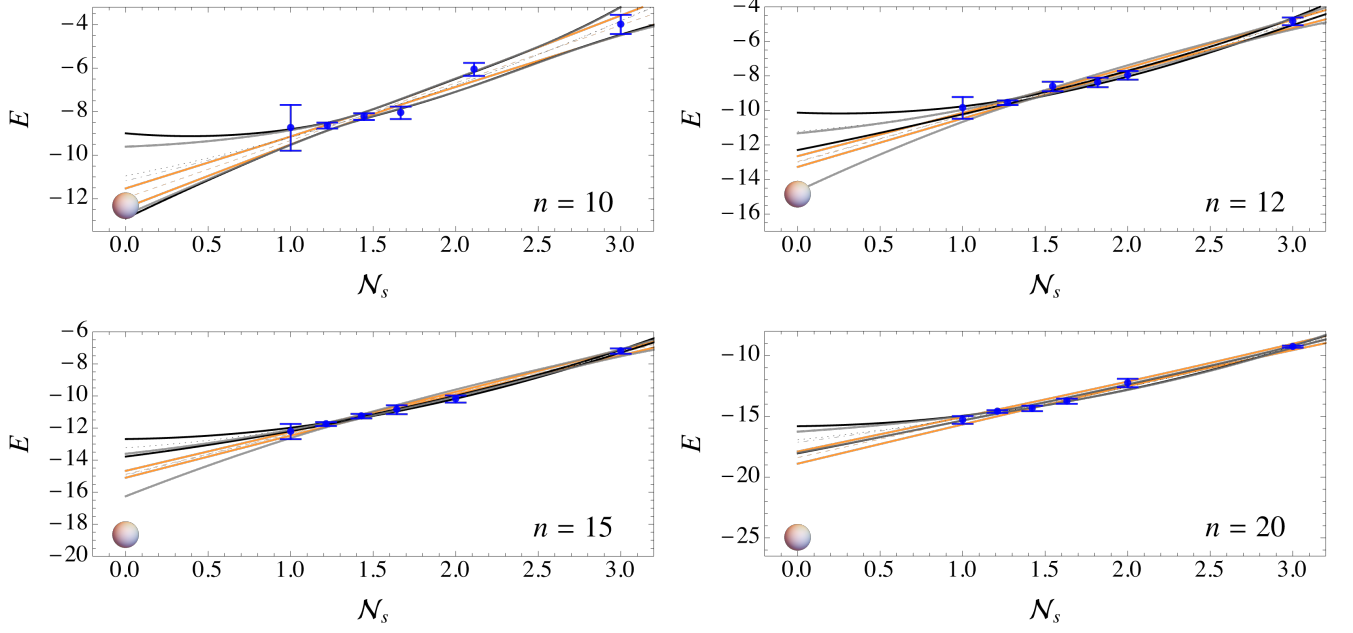


FIG. 14. Fitting results for different system size n , with light gray dot-dashed lines representing the exponential fit, black dashed lines for the quadratic fit, and the orange dashed line for the linear fit. The bands, bounded by solid lines, indicate the 68% confidence level (C.L.) uncertainties of the fits. The energies of the states prepared on the **Zuchongzhi** quantum chip at different values of \mathcal{N}_s are shown as blue circles, with statistical error bars. The white circle at \mathcal{N}_s indicates the energy of the state prepared by a noiseless quantum simulator.

CNOT gates in the circuit and $2n - 2$ is the minimum CNOT gates returned by FunSearch. The noise strengths \mathcal{N}_s considered for different n are shown in Fig. 14.

For $\mathcal{N}_s = 1$, the circuit corresponds to the original circuit. For noise strengths of 3, each CNOT gate in the original circuit is replaced by 3 CNOT gates, respectively. For the cases of $\mathcal{N}_s = 1, 3$, we only performed a single run for each. For the other noise strength cases with $\mathcal{N}_s < 3$, we randomly select the number of CNOT gates in the circuit and replace each selected CNOT gate with three CNOT gates to match the corresponding \mathcal{N}_s . To reduce statistical error, this process is repeated five times to generate five circuits, and the final result is obtained by averaging the outcomes of these five circuits.

For the original data, we use the jackknife method to compute the energy and standard error for each circuit. When the noise strength is not 1 or 3, we also apply the jackknife method to calculate the mean and standard error when averaging the results of the five circuits. Then, we fit the noise strength and energy to obtain the energy in the zero-noise limit. We consider three fits: a three-parameter exponential fit $E(\mathcal{N}_s) = a + b \exp(-c\mathcal{N}_s)$, a three-parameter quadratic fit $E(\mathcal{N}_s) = a + b\mathcal{N}_s + c\mathcal{N}_s^2$, and a two-parameter linear fit $E(\mathcal{N}_s) = a + b\mathcal{N}_s$. Fig. 14 shows the fitting results for different values of n .